Environment, Climate Change and Low Carbon Economy Programme

'Environment Programme'

European Economic Area (EEA) Financial Mechanism 2014-2021

A5 Report – Numerical assessment

28/07/2023

37_Call#2_Circular Construction in Energy-Efficient Modular Buildings

Accordingly, with the Articles 25.2.j) and 29.4 of the 'Applicants Guide for Financing of Projects Supported by Environment, Climate Change and Low Carbon Economy Programme'
https://www.eeagrants.gov.pt/media/2994/applicants-guide-for-financing-eea-grants_environment-projects_28112019.pdf

1. Introduction

This report presents the actions developed during activity A5 – Numerical assessment, which was performed between March 2022 and July 2023.

This activity was divided into three main actions:

- Hygrothermal assessment using WUFI Pro software;
- Thermo-mechanical assessment using ABAQUS software;
- Thermo-energetic assessment using DesignBuilder software, coupled with EnergyPlus.

Regarding the project indicator defined for A5, "Formulations analysed in numerical assessments", Circular2B increased the knowledge of the hygrothermal, thermo-mechanical and thermo-energetic impact through the four developed simulation models: two in WUFI Pro (2D models corresponding to two façade systems: SIP and ETICS), one in ABAQUS (façade 3D model) and another one in DesignBuilder (3D modular house).

2. Hygrothermal assessment

2.1. Framework and simulation model

The main objective of the present study was to evaluate the hygrothermal performance of the new SIP panel, incorporating the new core formulation (SIP (ART)) and comparing it with a

traditional SIP (SIP (EPS)) and the widely used ETICS (External Thermal Insulation Composite System), with EPS insulation.

Figure 1, Figure 2 and Figure 3 present the simulation models of the different façade systems with the same thermal transmission (U-value).

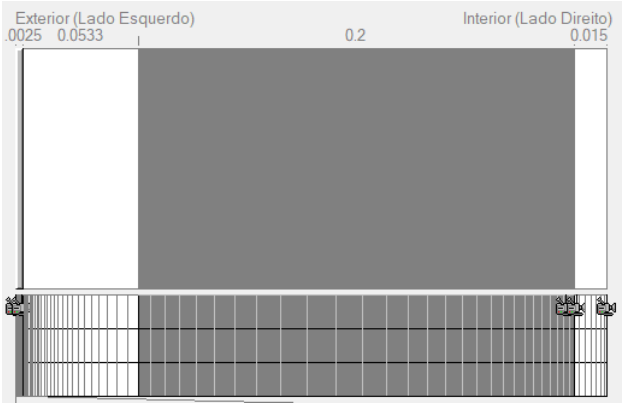

Figure 1: Simulation model of ETICS – Layers from exterior to interior: Base coat, EPS, lightweight concrete block and plaster.

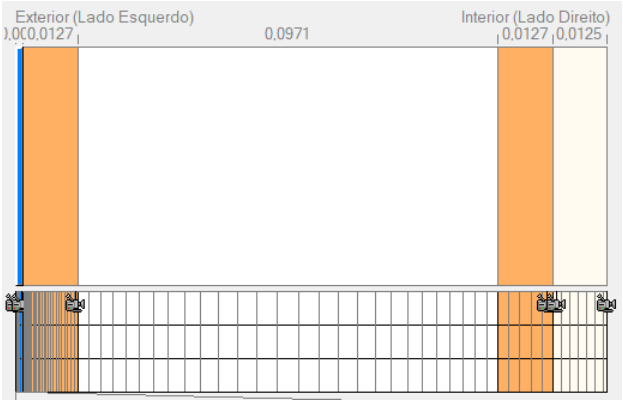

Figure 2: Simulation model of SIP (EPS) – Layers from exterior to interior: Permeable membrane, OSB, EPS, OSB and gypsum board.

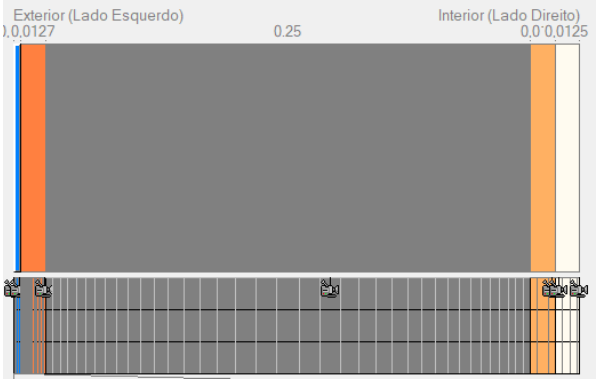

Figure 3: Simulation model of SIP (EPS) – Layers from exterior to interior: Permeable membrane, OSB, thermal insulation mortar, OSB and gypsum board.

Table 1 shows the material properties of all the materials that constitute the different façade systems. The core thermal insulation mortar (ART) properties were experimentally measured within the context of previously concluded master and doctoral theses.

Table 1: Material properties of the façade system layers.

Material properties	Base coat	EPS	Lightweight concrete block	Plaster	Permeable membrane	OSB	Gypsum board	Thermal insulation mortar (ART)
Thickness (m)	0.0025	0.06	0.20	0.015	0.001	0.0125	0.0125	0.25
Bulk density (kg/m^3)	1250	15	600	1450	1000	630	850	644
Porosity (m^3/m^3)	0.25	0.95	0.72	0.2	0.0002	0.6	0.65	0.76
Specific heat (J/kg.ºC)	1000	1500	850	1000	1000	1500	850	1111
Thermal conductivity (W/m.ºC)	0.45	0.04	0.14	0.61	1.00	0.13	0.2	0.103
Water vapour diffusion resistance factor (-)	12	30	8.3	10	150	650	8.3	8.7

A water vapour diffusion equivalent air thickness, corresponding to a fictitious finishing coating layer, of 0.61 (sd) was selected for the ETICS based on experimental literature values.

Table 2 shows the different combinations for the simulation scenarios, varying for each façade system the three solar absorption coefficients, two wall orientations and three climates.

Table 2: Simulation scenarios for the hygrothermal assessment.

Façade systems	Total thickness (m)	Solar absorption (-)	Emissivity (-)	Orientation	Climates
ETICS	0.271	0.27/0.59/0.88	0.9	North/South	Porto/ Bordeaux/Helsinki
SIP (EPS)	0.136				
SIP (ART)	0.289				

The values for solar absorption were acquired within the scope of a 2016 dissertation that conducted these measurements experimentally. Hence, three solar absorption coefficients were selected: 0.27 (white coating), 0.59 (green coating), and 0.88 (dark coating). The emissivity was set as 0.9 according to experimental measurements in the literature.

Regarding orientation, the South and North were chosen due to their higher and lower solar radiation exposure, respectively.

Given the considerable climatic diversity across Europe, three distinct climatic zones were selected to evaluate the hygrothermal performance of the previously described systems. These locations were chosen to offer a comprehensive analysis of the varying European climatic conditions, taking into account different geographical regions. Consequently, the climates of Porto (P) (Southern Europe, Figure 4), Bordeaux (B) (Central Europe, Figure 5), and Helsinki (H) (Northern Europe, Figure 6) were selected. Porto was chosen regarding its applicability in the South of Europe and also in relation to Circular2B. The prevalence of Cfb climates in Europe is the primary reason for selecting Bordeaux. Lastly, Helsinki was chosen due to its highly severe weather and strong inclination towards modular/sustainable construction.

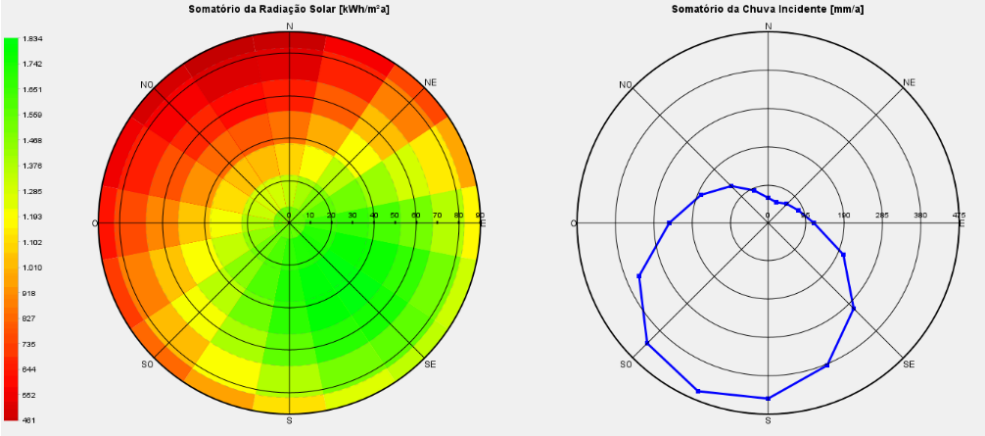

Figure 4: Solar radiation sum (left) and Driving rain sum (right) in Porto.

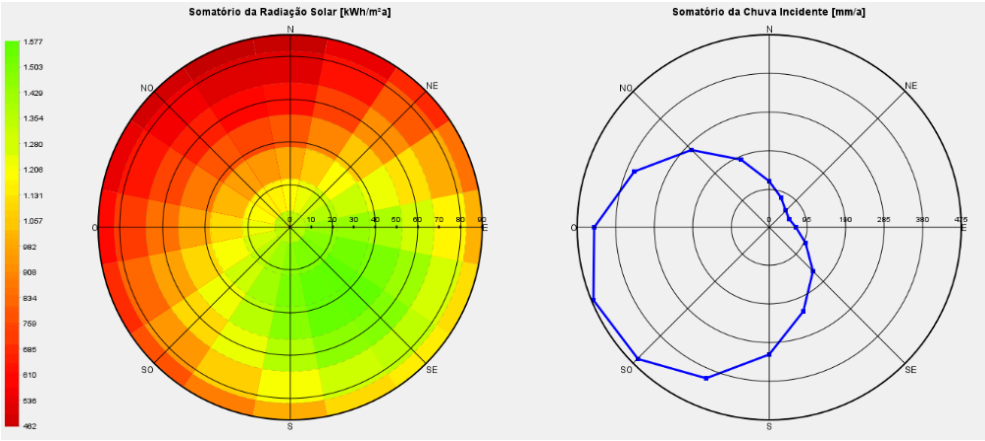

Figure 5: Solar radiation sum (left) and Driving rain sum (right) in Bordeaux.

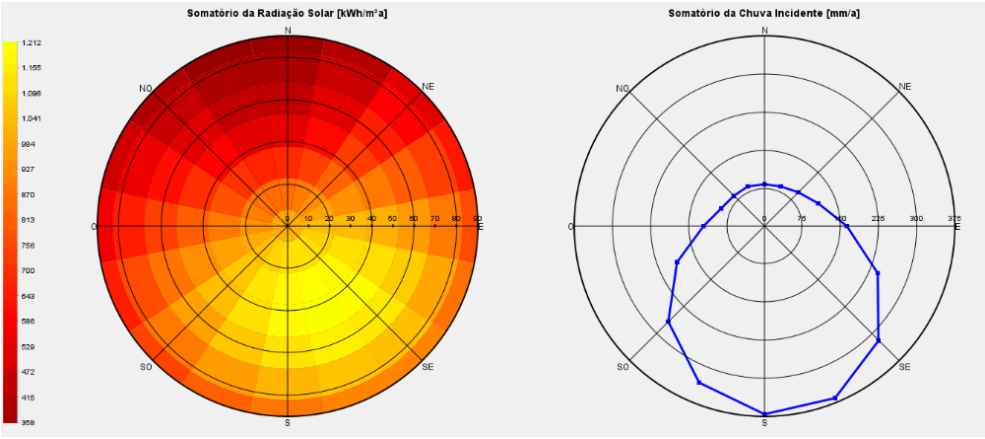

Figure 6: Solar radiation sum (left) and Driving rain sum (right) in Helsinki.

The influence of wind driving rain was not taken into consideration. The indoor climate was defined according to sine wave curves, with an average temperature of 21°C and relative humidity of 50%. These scenarios were simulated for one year.

2.2. Influence of the façade system type on hygrothermal behaviour

The hygrothermal behaviour of the three different façades systems was evaluated considering the two extreme solar absorptions (0.27 and 0.88) and Porto climate. The hygrothermal indicators are the water content (total and on the insulation layer), exterior surface temperature and exterior surface condensation potential.

Figure 7 a) and b) show the total water content for the three simulated façade systems considering North and South orientation, respectively.

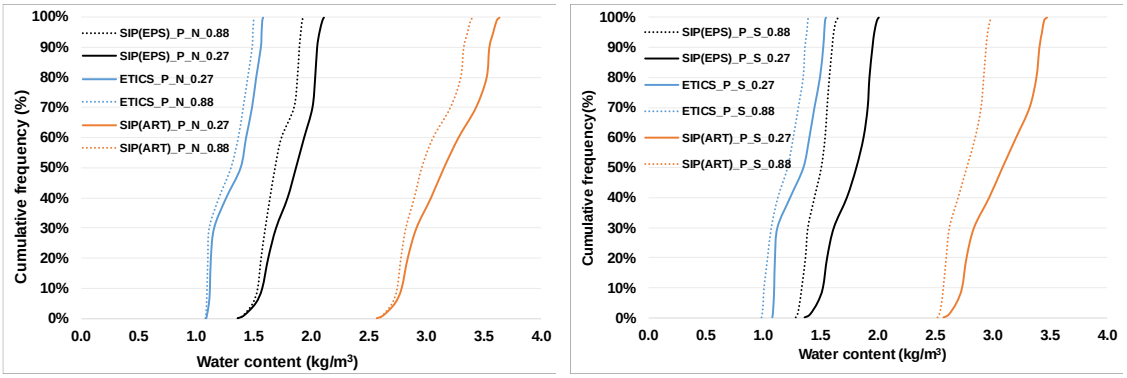

a) b)

Figure 7: Influence of the façade system – water content a) North and b) South.

As can be observed, the systems with EPS as thermal insulation present, as expected, a lower water content than SIP (ART). That difference may be attributed to SIP(ART) having a water saturation content of around 320 kg/m^3, significantly higher than the EPS, which is almost waterproof. Also, the North-oriented façades presented higher water content, especially for light colours. The use of dark coatings contributed to lower water content, which could be related to the drying effect boosted by the higher surface temperature. Also, these dark coatings resulted in smaller water content variations, mainly in the South façade.

Figure 8 a) and b) show the water content in the thermal insulation layer for the three simulated façade systems considering North and South orientation, respectively.

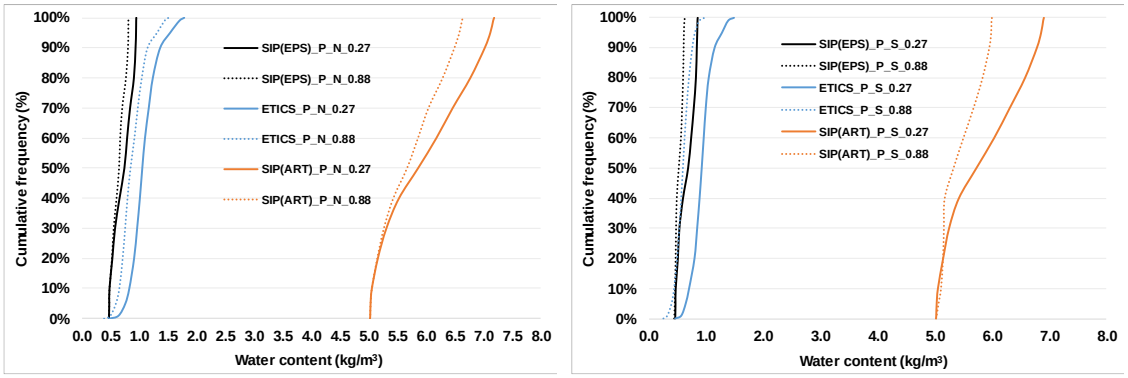

a) b)

Figure 8: Influence of the façade system – water content in the thermal insulation layer a) North and b) South.

Again, the façade systems with EPS presented very low water content values. An increase in moisture content is approximately five times higher in SIP(EPS) compared to SIP(ART).

Figure 9 a) and b) show the exterior surface temperature for the three simulated façade systems considering North and South orientation, respectively.

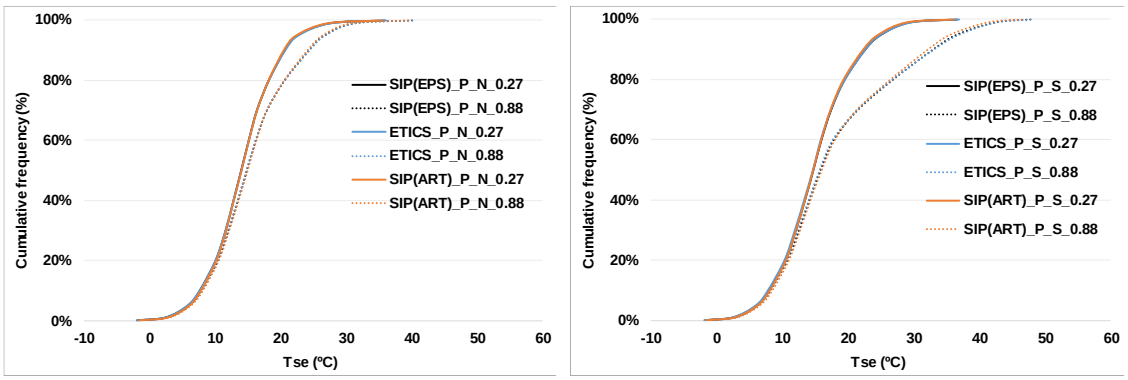

a) b)

Figure 9: Influence of the façade system – exterior surface temperature a) North and b) South.

Comparing the façade systems with EPS, no significant variation was observed between the systems for a solar absorption of 0.27 and across different orientations. The maximum difference did not exceed 1°C. The highest recorded temperatures were 36.9°C for the ETICS and 36.6°C for

the SIP(EPS), The lowest temperatures recorded were -1.9°C for the ETICS and the SIP(EPS), with no discernible variation observed between the north and south orientations. Similarly, no notable variation was observed for a solar absorption of 0.88. The maximum recorded temperatures were 48.0°C for the ETICS and 47.8°C for the SIP(EPS) in the south orientation. However, for the north orientation, there is a reduction of approximately 8°C in both systems, as in the previous scenario.

Comparing the SIPs, no significant disparities in exterior surface temperature exist for the same solar absorption coefficient. However, a slight phase shift is noticeable between the absorption coefficients of 0.27 and 0.88. In the south orientation, a phase shift of approximately 1°C is observed, and this disparity magnifies at higher temperatures. Consequently, across all instances, the phase shift averages around 7°C. For 50%/60% of occurrences, the exterior surface temperature exhibits minimal divergence between the two orientations. Nonetheless, beyond the 60% threshold, this phase shift significantly amplifies, particularly evident on darker surfaces. Thus, the north orientation demonstrates a more consistently stable behaviour, even amidst substantially distinct colour variations, in contrast to the southern façade.

It can be concluded that the exterior surface temperature is not influenced by the type of system employed but rather by the variation in the solar absorption coefficient, i.e., by the surface properties of the thin coating layer.

Figure 10 a) and b) show the exterior surface condensation potential for the three simulated façade systems considering North and South orientation, respectively.

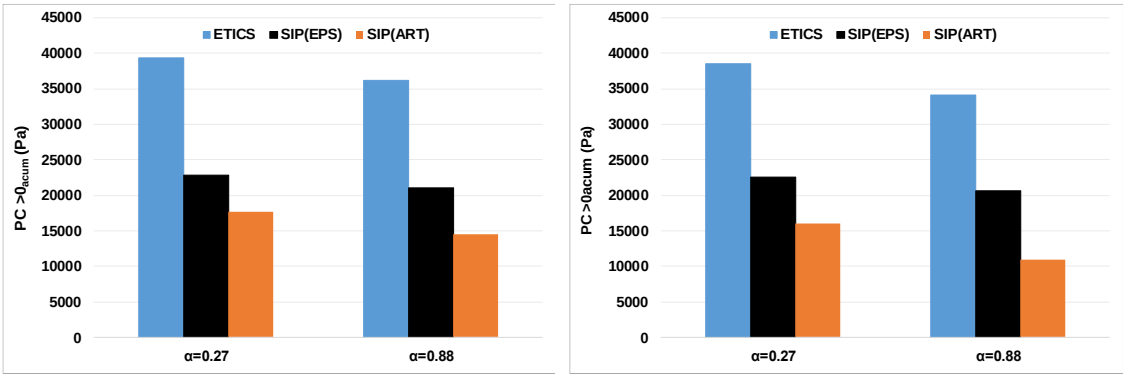

a) b)

Figure 10: Influence of the façade system – exterior surface condensation potential a) North and b) South.

The reduction in condensation potential for the southern orientation, comparing ETICS with SIP(EPS), was approximately 41.5% for α=0.27 and 40% for α=0.88. The reduction was about 42% for the northern orientation for α=0.27 and nearly the same for both southern and α=0.88 orientations. The 40% reduction between systems can be attributed to the difference in material effusivity between the two systems.

While both systems share the same thermal insulation (EPS) and possess the same thermal effusivity of EPS, the significant disparity lies in the materials adjacent to the EPS. In the case of ETICS, the material adjacent to the outer side is the base coat, which has an effusivity of 750 $Wm^{-2}K^{-1}s^{-1/2}$. In the case of SIP(EPS), the adjacent material consists of an OSB board and a permeable membrane with effusivity values of 358.20 $Wm^{-2}K^{-1}s^{-1/2}$ and 1000 $Wm^{-2}K^{-1}s^{-1/2}$, respectively. Consequently, the SIP(EPS) materials exhibit higher effusivity than those comprising ETICS, implying that the material possesses a greater capacity to absorb and release heat to its surrounding environment. This, in turn, facilitates enhanced heat supply to the surface, thereby mitigating the phenomenon of nocturnal overcooling (condensation potential on the exterior surface).

Comparing SIP(EPS) with SIP(ART), a notably more significant variation is observed for the northern orientation. The reduction in CP is approximately 40.3% for a solar absorption coefficient of 0.27 (light colour) and 46.2% for 0.88 (dark colour). The decrease in CP for the southern orientation is approximately 45% for an absorption of 0.27 and 59% for an absorption of 0.88. Properties such as effusivity influence the SIP(ART) system to possess a higher capacity to absorb and release heat to its surroundings than SIP(EPS), thus diminishing the potential for condensation, as explained before.

2.3. Influence of the exterior coating on the hygrothermal behaviour of façade systems

The impact of the finishing coatings on the hygrothermal behaviour of the three different façades systems was evaluated considering the three solar absorption coefficients (0.27, 0.59 and 0.88) and Porto climate, with the exterior surface temperature as the hygrothermal indicator. This indicator was explored in-depth for the entire simulation period and the hottest and coldest weeks of the year.

Figure 11 a) and b) show the exterior surface temperature for the three simulated façade systems considering North and South orientation, respectively.

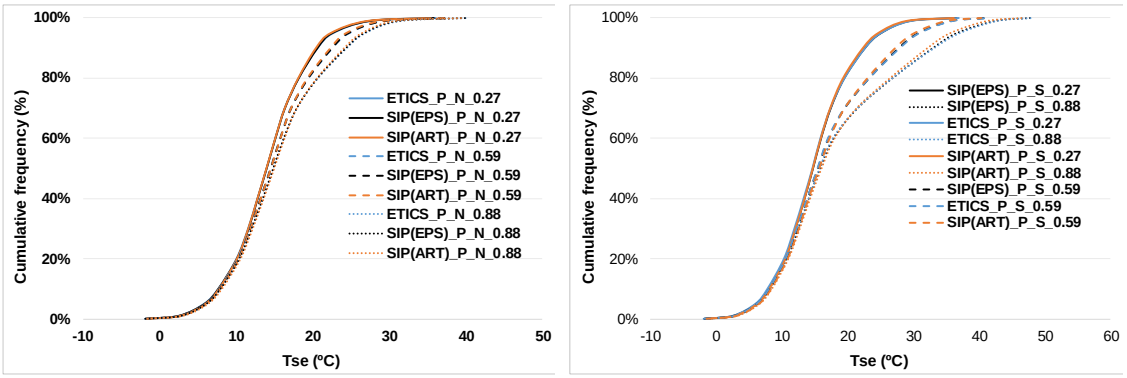

a) b)

Figure 11: Influence of the finishing coating – exterior surface temperature a) North and b) South.

Once again, it is evident that no significant variation in exterior surface temperature exists between systems with the same solar absorption coefficient. All systems with a solar absorption coefficient of 0.59 exhibit higher maximum temperature values than all systems with 0.27 and lower temperature values than those with 0.88. Therefore, as expected, the behaviour resembles that observed with other absorption values, falling predictably between the extremes. It is also noteworthy that there is a more significant difference between the systems for maximum temperature values in the southern orientation.

To comprehend system behaviour during winter and summer, the subsequent subchapters present analyses for the warmest and coldest weeks of the year.

Subsequently, the SIP systems will be comprehensively evaluated. Figure 12 a) and b) portray the variation of Tse (exterior surface temperature) between SIP(EPS) and SIP(ART) for the warmest week of the year, considering the south and north orientations, respectively.

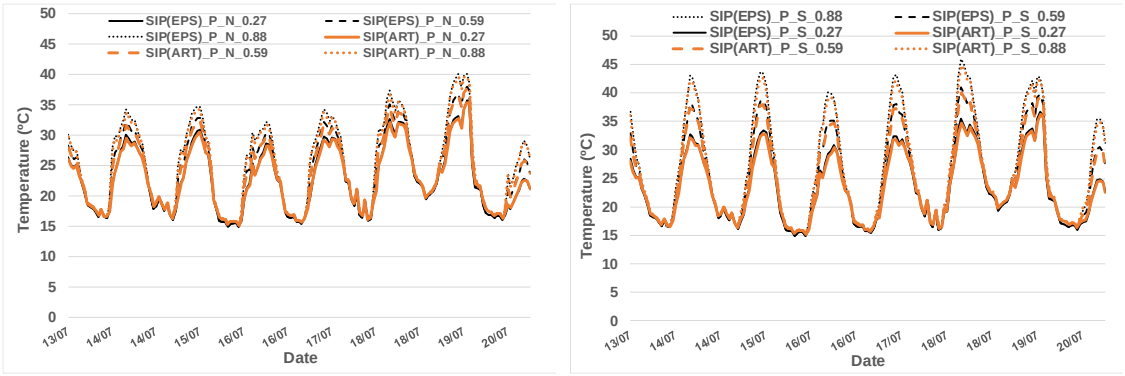

a) b)

Figure 12: Exterior surface temperature during the hottest week a) North and b) South.

While the graphs are identical for both north and south orientations, there is a more pronounced disparity between systems with different absorption coefficients in the south orientation. In this case, the SIP(EPS) and SIP(ART) systems with a solar absorption value of 0.88 exhibit significantly higher values than systems with absorption values of 0.59 and 0.27. In the north-facing façade, this disparity also exists, but it is much less pronounced compared to the south orientation. Naturally, systems with a solar absorption of 0.88 absorb more solar radiation, resulting in a higher maximum exterior surface temperature compared to systems with lower absorption values. For systems with a solar absorption coefficient of 0.59 and systems with coefficients of 0.27 and 0.88, the minimum temperature attained hovers around 14.8 ºC for SIP(EPS) and 15.2 ºC for SIP(ART). Despite the nearly identical, the SIP(ART) system does not cool down as much as SIP(EPS), which may be related to thermal inertia playing a role. It can also be concluded that the minimum Tse undergoes minimal significant changes with varying solar orientation, solar absorption coefficient, and system type.

Regarding the maximum temperature reached by the systems during the analysed week, in the south orientation, the SIP(EPS) system achieved a slightly higher temperature than SIP(ART), with a difference of approximately 1°C for the south orientation and about 0.5°C for the north orientation. Thus, it can be observed that there is a more significant variation in maximum exterior surface temperature between different solar absorption coefficients in the south orientation. In contrast, in the north façade, the difference between systems with distinct absorption coefficients is minimal. This variation can be attributed to a higher incidence of solar radiation in the south orientation compared to the north orientation, as previously mentioned.

Figure 13 a) and b) show the variation of Tse between SIP(EPS) and SIP(ART) for the coldest week of the year, considering the south and north orientations, respectively.

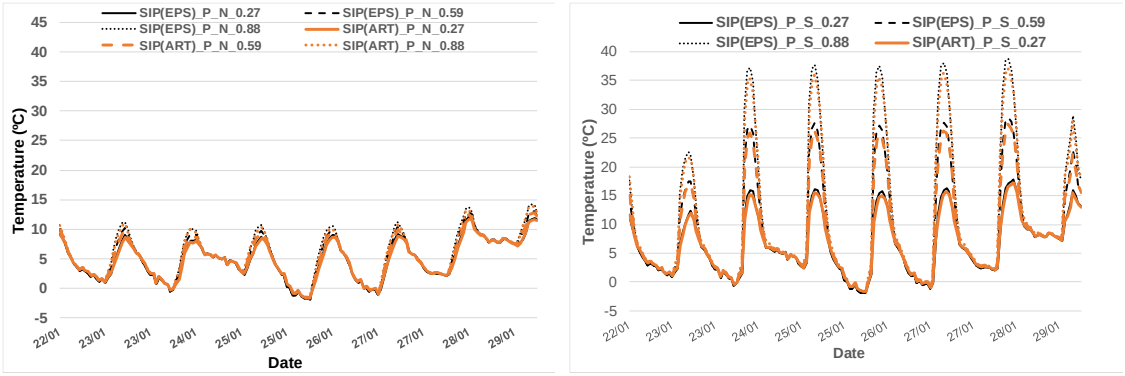

a) b)

Figure 13: Exterior surface temperature during the coldest week a) North and b) South.

Once again, the high incidence of solar radiation on the south-facing façade implies that systems with higher solar absorption coefficients (0.59 and 0.88) attain elevated exterior surface temperatures, consequently resulting in larger thermal amplitudes. In contrast, the low solar radiation incidence on the north-facing façade implies that systems with solar absorption coefficients of 0.59 and 0.88 have a much smaller impact on the variation of Tse, leading to significantly reduced thermal amplitudes.

The variation of Tse for the south orientation exhibits more disparate values than the north orientation. The maximum recorded exterior surface temperature for the south orientation and solar absorption of 0.59 during the coldest week was 28.6°C for SIP(EPS) and 27.4°C for SIP(ART). For the north-facing façade, the maximum Tse was 12.9°C for SIP(EPS) and 12.8°C for SIP(ART). Observing these values, it becomes evident that under identical orientation, location, and solar absorption conditions, the SIP(EPS) system registers higher maximum Tse values than SIP(ART). The minimum recorded exterior surface temperature was -1.9°C for SIP(EPS) and -1.5°C for SIP(ART) for the south-facing façade. For the opposite-facing façade, the minimum Tse was -2.2°C for SIP(EPS) and -1.6°C for SIP(ART). Hence, the minimum Tse values obtained by the SIP(EPS) system are slightly lower than those of SIP(ART). Consequently, the SIP(EPS) system achieves higher maximum exterior surface temperatures and lower minimum Tse values than SIP(ART).

Furthermore, the thermal amplitude of SIP(EPS) is greater than that of SIP(ART). For instance, for the SIP(EPS) system with a solar absorption coefficient of 0.59, the amplitude is 30.6 °C for the south orientation and 15.0 °C for the north orientation, respectively. In contrast, the amplitude for the SIP(ART) system is 28.9°C for the south orientation and 14.4 °C for the north orientation, respectively.

2.4. Influence of the climate conditions on the hygrothermal behaviour of façade systems

The impact of the climatic conditions on the hygrothermal behaviour of the three different façades systems was evaluated considering the two extreme solar absorptions (0.27 and 0.88) and the three climates – Porto, Bordeaux and Helsinki. The hygrothermal indicators are the total water content, exterior surface temperature, thermal lag and exterior surface condensation potential.

Figure 14 and Figure 15 show the total water content for the three simulated façade systems considering North and South orientation and 0.27 and 0.88 solar absorption coefficients, respectively.

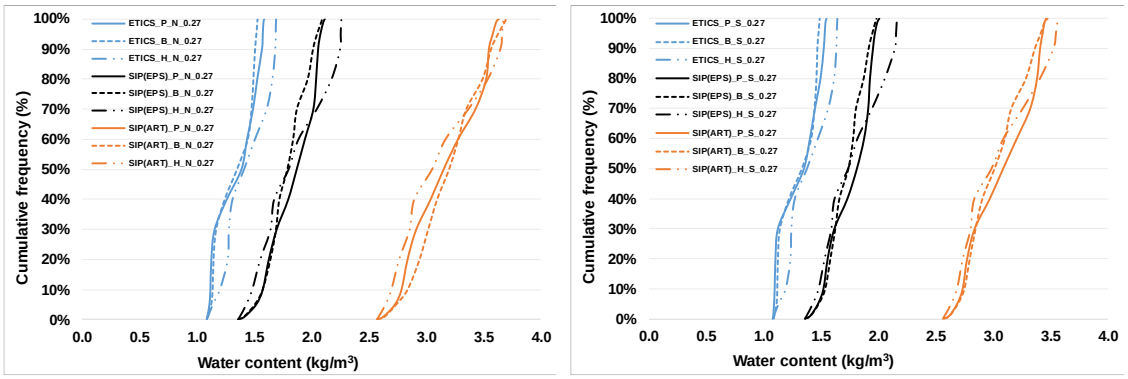

a) b)

Figure 14: Influence of the climate – total water content, solar absorption of 0.27 a) North and b) South.

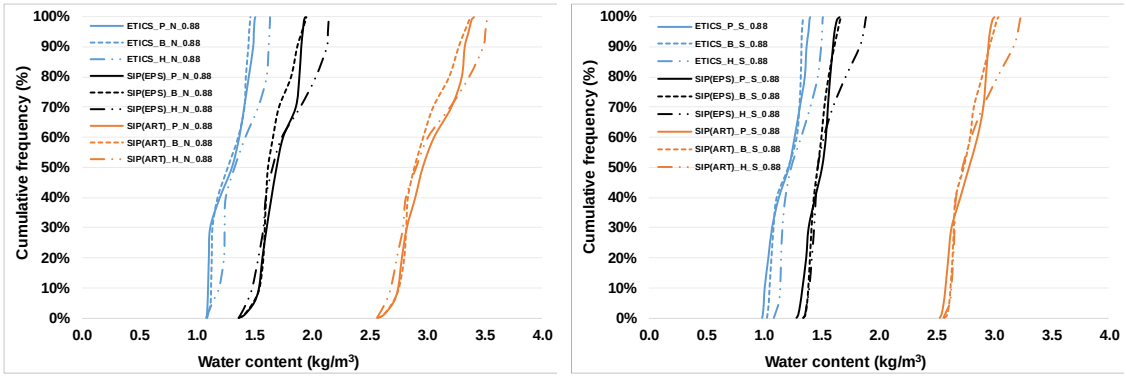

a) b)

Figure 15: Influence of the climate – total water content, solar absorption of 0.88 a) North and b) South.

In a general overview, for a solar absorption coefficient of 0.27 and the north orientation, there is an increase of 35% in the average total moisture content between ETICS and SIP(EPS) systems in the city of Porto, 34% in Bordeaux, and 29% in Helsinki. Examining the moisture content solely for the ETICS systems reveals slightly higher values in Helsinki than in other climates. Conversely, for the SIP(EPS) systems, Helsinki's climate and 50% of occurrences (i.e., 6 months of the year), the total moisture content is lower than that of Porto and Bordeaux. However, upon comparing these systems, the SIP(EPS) exhibits higher moisture content. The variation in moisture content is more significant for the north orientation compared to the south, as expected.

Considering a comprehensive analysis, for a solar absorption coefficient of 0.88 and the north orientation, there is a 32% increase in the average total moisture content between ETICS and SIP(EPS) systems in the city of Porto, 31% in Bordeaux and 27% in Helsinki. In comparison, there is a shift in the values mentioned in the south orientation, with an 8% increase for Porto, 6% for Bordeaux, and 5% for Helsinki.

Analysing the moisture content solely for the SIP(EPS) systems reveals slightly higher values in Helsinki compared to other climates. Conversely, for the SIP(ART) systems in Helsinki and north oriented-façade, the total moisture content is lower than that of Porto and Bordeaux in 70% of occurrences. For the south orientation, the total moisture content is lower for only 60% of occurrences. Despite this, the SIP(ART) presents higher moisture content when comparing these systems.

For a solar absorption coefficient of 0.88 and the north orientation, the average total moisture content between SIP(EPS) and SIP(ART) considerably increases: 77% in Porto, the same value for Bordeaux, and 73% in Helsinki. SIP(EPS) reveals slightly higher values in Helsinki compared to other climates. Conversely, for a higher solar absorption coefficient and between SIP(ART) systems, for the climate of Helsinki, north orientation, and 30% of occurrences (i.e., 4 months of the year), the total moisture content is lower than that of the same system but for the climates of Porto and Bordeaux. There is no significant variation in SIP(ART) systems for the south orientation for different climates. Despite this, as demonstrated in previous chapters, the SIP system with mortar consistently exhibits higher moisture content. It is possible to correlate this value and understand that the difference in moisture content between SIP(EPS) and SIP(ART) systems diminishes with increasing latitude.

Figure 16, Figure 17 and Figure 18 depict the exterior surface temperatures and surface temperatures on the gypsum board for SIP(EPS) and SIP(ART) on the day recorded with the highest external surface temperature with a solar absorption of 0.88, in the south orientation, for Porto, Bordeaux, and Helsinki, respectively.

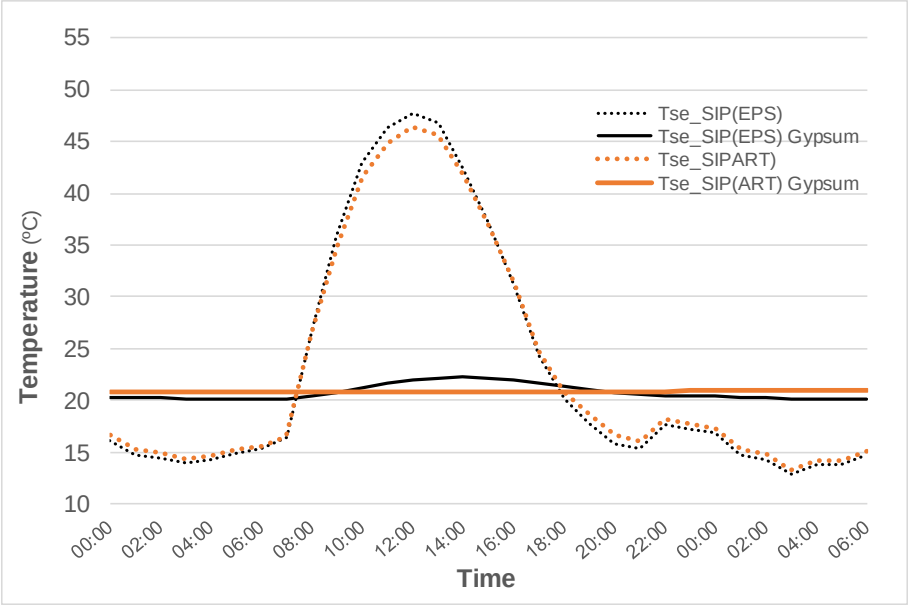

Figure 16: Influence of the climate – surface temperatures with solar absorption of 0.88 and South orientation in Porto

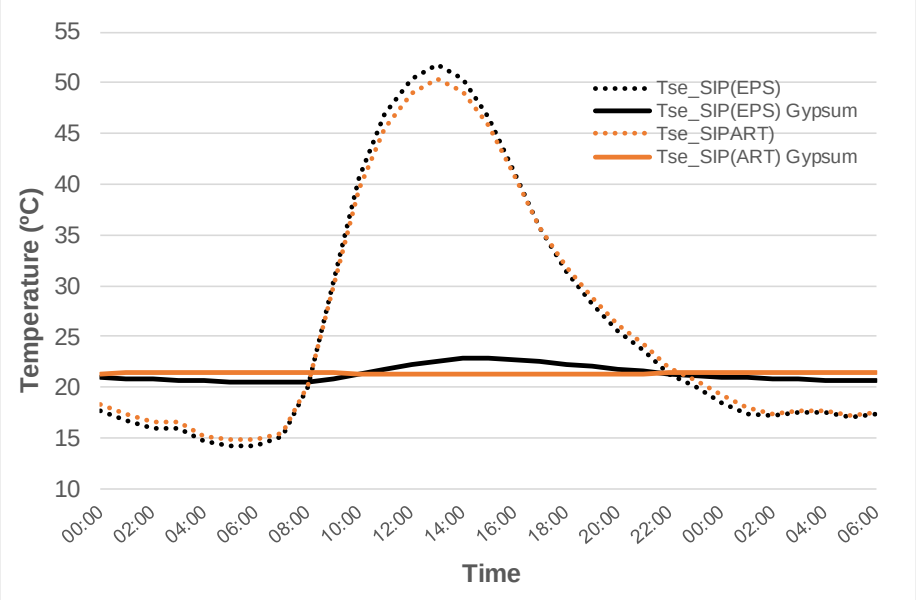

Figure 17: Influence of the climate – surface temperatures with solar absorption of 0.88 and South orientation in Bordeaux.

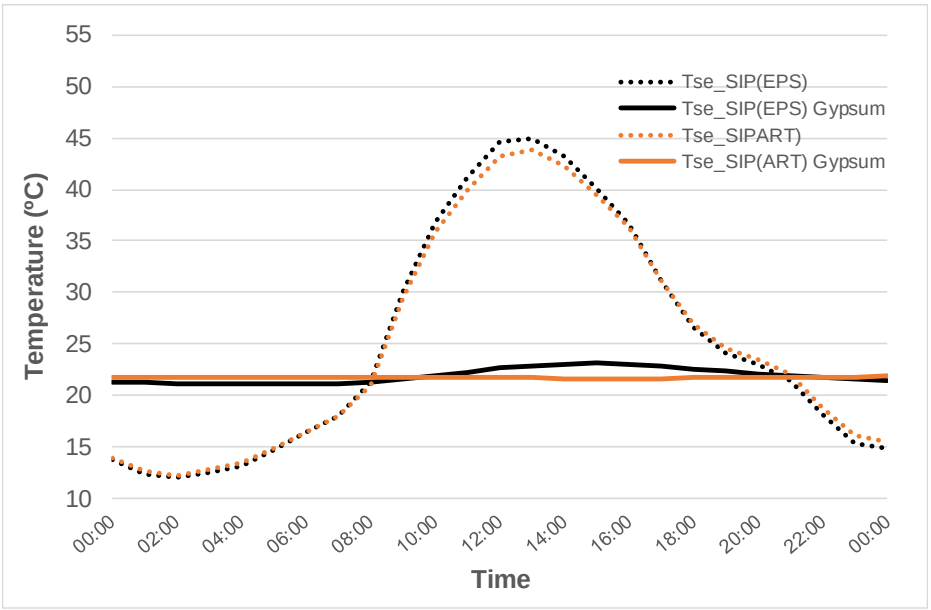

Figure 18: Influence of the climate – surface temperatures with solar absorption of 0.88 and South orientation in Helsinki.

In Porto, regarding Ts (Gypsum Board), a higher oscillation is observed for the EPS-core system, while the mortar-based SIP exhibits a more consistent temperature and lower oscillation. The time interval required for the system to reach maximum temperature in the innermost layer is 1

hour, whereas SIP(ART) reaches maximum temperature after 12 hours. Therefore, the thermal delay of a SIP(ART) system with α=0.27 is 11 hours, while for the same system with α=0.88, it is 12 hours.

In Bordeaux, the time interval required for the system to reach maximum temperature in the innermost layer is 2 hours, while SIP(ART) reaches maximum temperature after 16 hours. The amplitude in the SIP(EPS) gypsum layer is much higher than that of SIP(ART). This highlights the temperature stabilisation of the SIP(ART) interior compared to SIP(EPS), attributed to higher thermal inertia.

In Helsinki, the time interval required for the system to reach maximum temperature in the innermost layer is 1 hour for a light colour and 2 hours for a dark colour. In contrast, SIP(ART) reaches maximum temperature after 16 hours for both solar absorptions. The amplitude in the SIP(EPS) gypsum layer is 0.8 ºC for α=0.27 and 1.9 ºC for α=0.88, much higher than the amplitude values of SIP(ART). This underscores the temperature stabilisation of the SIP(ART) interior compared to SIP(EPS) due to higher thermal inertia.

One of the reasons for this thermal delay is the diffusivity of the core mortar compared to a system composed of EPS. Therefore, the lower the thermal diffusivity of a material, the longer it takes for different system layers to reach thermal equilibrium. Consequently, SIP(ART) exhibits a more significant thermal delay than SIP(EPS). Furthermore, for climates in Bordeaux and Helsinki, the thermal delay is greater than in Porto. In warmer Southern European climates, higher thermal inertia can contribute to reducing interior temperatures. The delay is shorter in Porto, emphasising the significance of reaching maximum interior temperature more rapidly in such climates.

Figure 19 and Figure 20a) and b) show the exterior surface condensation potential for the three simulated façade systems considering North and South orientation, for 0.27 and 0.88 solar absorption coefficients, respectively.

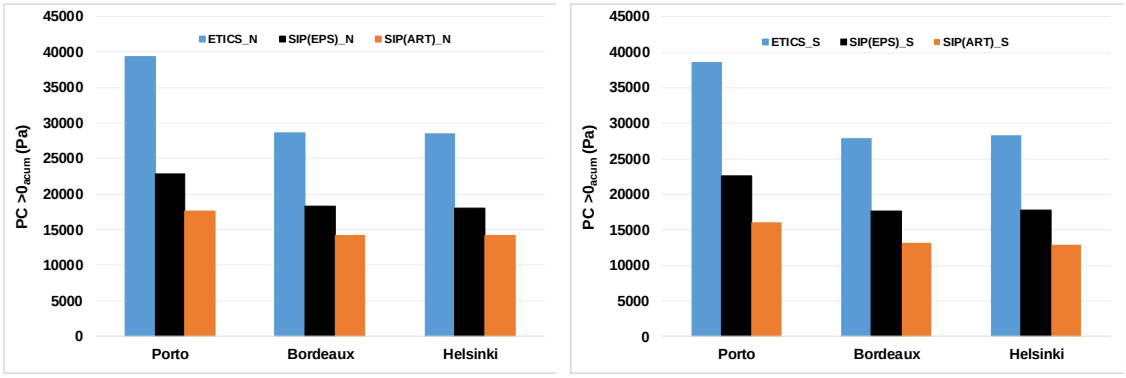

a) b)

Figure 19: Influence of the climate – exterior surface condensation potential, solar absorption of 0.27 a) North and b) South.

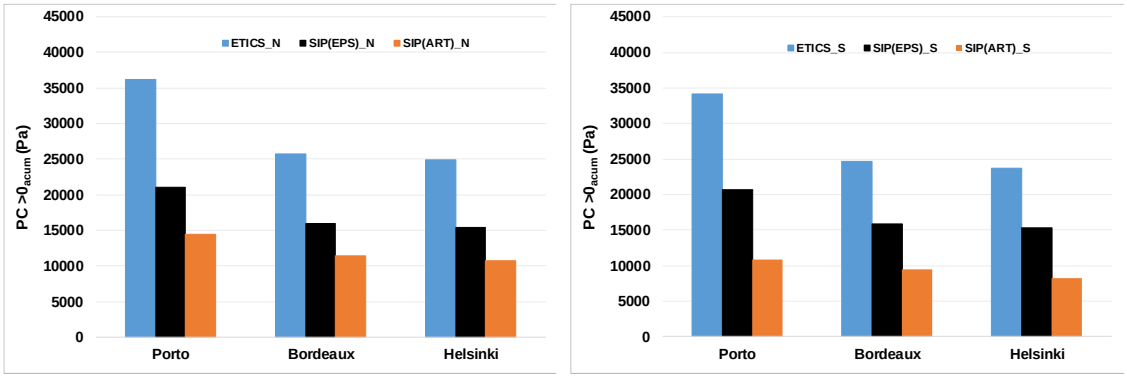

a) b)

Figure 20: Influence of the climate – exterior surface condensation potential, solar absorption of 0.88 a) North and b) South.

Comparing SIP(ART) to SIP(EPS) for the north orientation, the condensation potential for a solar absorption of 0.27 exhibits a reduction of approximately 22% for Porto, Bordeaux, and Helsinki. For the south orientation, as expected, the reduction in CP is greater, at 29% for Porto, 26% for Bordeaux, and 27% for Helsinki. The Porto climate presents relatively higher accumulated values than Bordeaux and Helsinki in absolute values. The Helsinki climate displays the lowest total value of CP for both north and south orientations. This result may be attributed to the climate, which relies heavily on the exterior temperature, high exterior relative humidity, and exterior surface temperature. Once again, the SIP(ART) system's higher effusivity leads to slower cooling compared to SIP(EPS), thereby decreasing the potential for condensation. It can be concluded that this phenomenon holds for all climates under study, with a more pronounced reduction observed for the Porto climate.

Comparing SIP(ART) to SIP(EPS) for the north orientation, the condensation potential for a solar absorption of 0.88 reduces CP by approximately 31% for Porto, Bordeaux, and Helsinki. For the south orientation, as expected, the reduction in CP is greater, at 47% for Porto, 40% for Bordeaux, and 48% for Helsinki. It can be concluded that a SIP(ART) system with a darker colour has a more noticeable reduction in condensation potential compared to a system with a white colour. Notably, in absolute values, the Porto climate presents relatively higher accumulated values compared to Bordeaux and Helsinki.

The significant reduction in CP from SIP(EPS) to SIP(ART) is attributed to the higher thermal effusivity of the mortar core compared to the EPS core. This greater thermal effusivity implies that the material has a greater capacity to absorb and release heat to the surrounding area, facilitating a higher heat supply to the surface and thus reducing the potential for condensation.

3. Thermo-mechanical assessment

3.1. Framework and simulation model

The main objective of the present analysis was to evaluate the influence of the substrate in the development of stresses in thermal insulation mortars.

ABAQUS software, from *Dassault Systémes*, is a thermo-mechanical simulation tool that allows reproducing heat transfer problems using the finite element method. The coupled thermo-mechanical analysis is performed by the combination of, at first, thermal analysis and, then, the stress/strain mechanical analysis.

A 3D model of 2.5x3.0 m^2 was designed. Boundary constraints, in terms of displacements and rotations, were defined as:

- Displacements in x*yz*-axis blocked: base of the wall;
- Displacements in the z-axis blocked: top and sides of the wall.

Figure 21 presents the schematic 3D model used in the thermo-mechanical simulation, corresponding the front layer to the exterior surface.

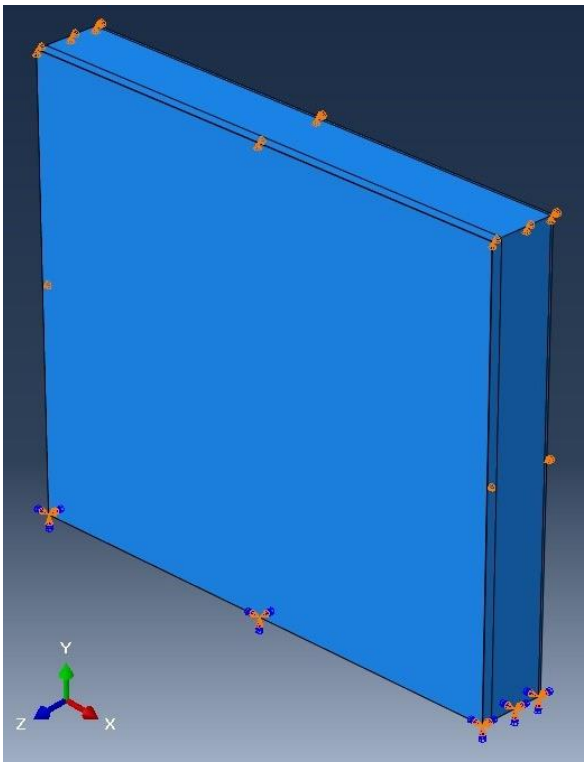

Figure 21: 3D simulation model constitution: base coat, thermal insulation mortar, substrate and plaster, from left (exterior) to right (interior).

The material properties used as input for the thermo-mechanical simulation were obtained in the WUFI Pro Database and bibliography references, as presented in Table 3. Three different substrates of aerated concrete blocks, standard ceramic bricklayer and oriented strand board (OSB) with current thicknesses were compared. The effect of the thermal shock (abrupt decrease of temperature 70 to 15 ºC) with the different substrates combined with the thermal rendering system and the plaster is analysed.

The comparison between different substrates allows for analysing the effect of using a current substrate configuration (heavy construction) or a lightweight substrate, evaluating the influence of distinct rigidities.

Table 3: Material properties for thermo-mechanical simulation.

Layer		Thickness (m)	ρ (kg/m³)	λ (W/m.ºC)	a' (x10-6/ºC)	E (MPa)	c (J/kg.ºC)	υ (-)
Exterior	**Base coat**	**0.004**	**1197.0**	**0.2202**	**9.6**	**3820.6**	**900**	**0.17**
Insulation	Thermal insulation mortar	0.060	208.7	0.0487	9.0	103.5	1000	0.20
Substrate alternatives	Aerated concrete	0.260	600.0	0.1400	10.8	2125	850	0.20
	Brick masonry	0.150	650.0	0.5500	4.5	1600	850	0.25
	OSB	0.025	630.0	0.1200	7.0	7500	850	0.15
Interior	Plaster	0.015	850.0	0.2000	17.0	3500	850	0.20

3.2. Results and discussion

The typical deformed shape and principal stresses after heating and after the abrupt decrease are shown in Figure 22 and Figure 23.

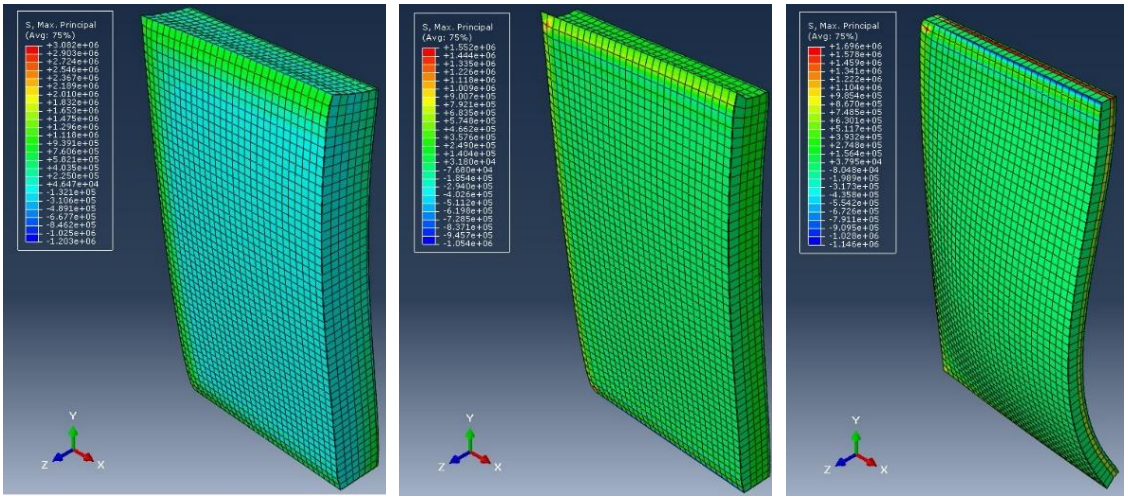

a) b) c)

Figure 22: Typical deformed shape after heating, using: a) Aerated concrete; b) Brick masonry; c) OSB.

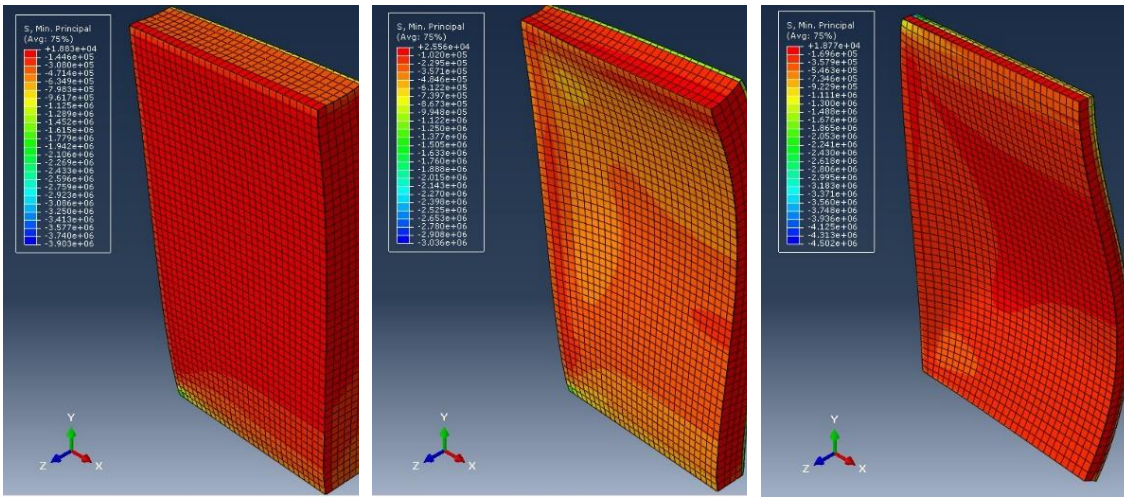

a) b) c)

Figure 23: Typical deformed shape after the abrupt decrease, using: a) Aerated concrete; b) Brick masonry; c) OSB.

The higher curvature of walls using thinner substrates, especially the OSB, can be seen in both expansion and contraction periods. This fact induces higher deformation and the high rigidity of the OSB promotes the increase of stresses, as shown in the following results.

Table 4 and Table 5 present the maximum stresses and displacements, respectively, after heating (70 ºC) and after the abrupt decrease (15 ºC), considering the three different substrates in the thermal insulation mortar surfaces (exterior and interior), in a central node of the wall.

Table 4: Tensile and compressive stresses obtained in the thermal insulation layer surfaces with different substrates.

Substrate	Tensile stress (ext/int) (Pa)	Compressive stress (ext/int) (Pa)
	T=70 ºC	T=15 ºC
Aerated concrete	2554.7/1363.9	-1332.6/-380.4
Brick masonry	788.2/335.2	-353087.0/-8832.0
OSB	4677.4/849.1	-58432.7/-2021.9

Table 5: Displacements obtained in the thermal insulation layer surfaces with different substrates.

Substrate	Displacements (ext/int) (m)	
	T=70 ºC	T=15 ºC
Aerated concrete	8.13/7.90x10-4	3.68/3.70x10-4
Brick masonry	3.46/3.54x10-4	3.74/3.57x10-4
OSB	9.46/9.25x10-4	5.36/5.35x10-4

The type of substrates significantly impacted the thermal shock effect in exterior thermal rendering systems. The OSB's low thickness and the panel's high rigidity results in more significant displacements in the thermal insulation layer at high and low temperatures (thermal shock). Regarding the tensile stresses, the higher the rigidity of the substrate, the higher the stresses in the thermal insulation mortar, as shown in Figure 24.

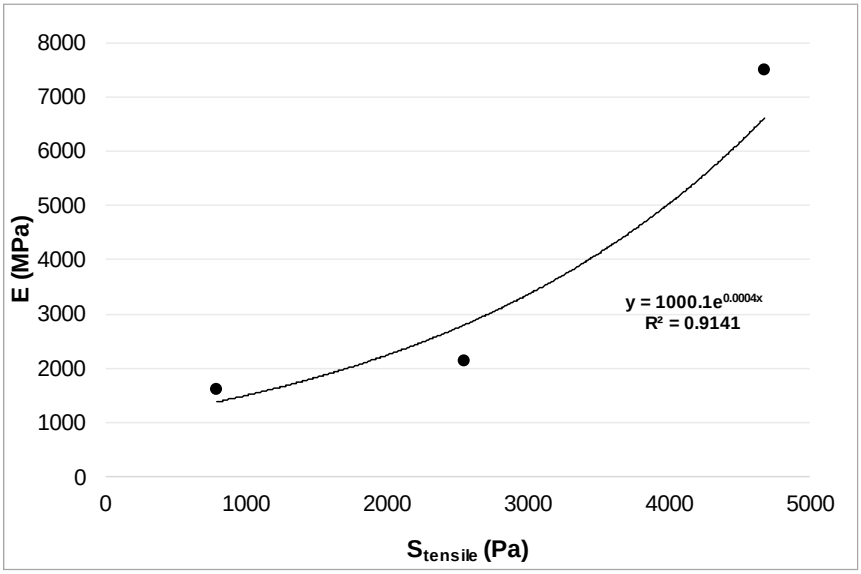

Figure 24: Tensile stresses in the thermal insulation mortar as a function of the elastic modulus of the substrate.

The aerated concrete and the OSB substrates promote higher displacements regarding the expansion period, which follows the higher thermal expansion coefficients compared to the brick masonry. In addition, the aerated concrete and OSB substrates promote higher stresses in the inner surface of the thermal insulation mortar, as shown in Figure 25, especially using the aerated concrete with the highest thermal expansion coefficient.

However, analysing the profile of the strain distribution, the aerated concrete substrate resulted in a more homogeneous distribution than brick masonry and OSB, which allows better compatibility between the different layers, as shown in Figure 26.

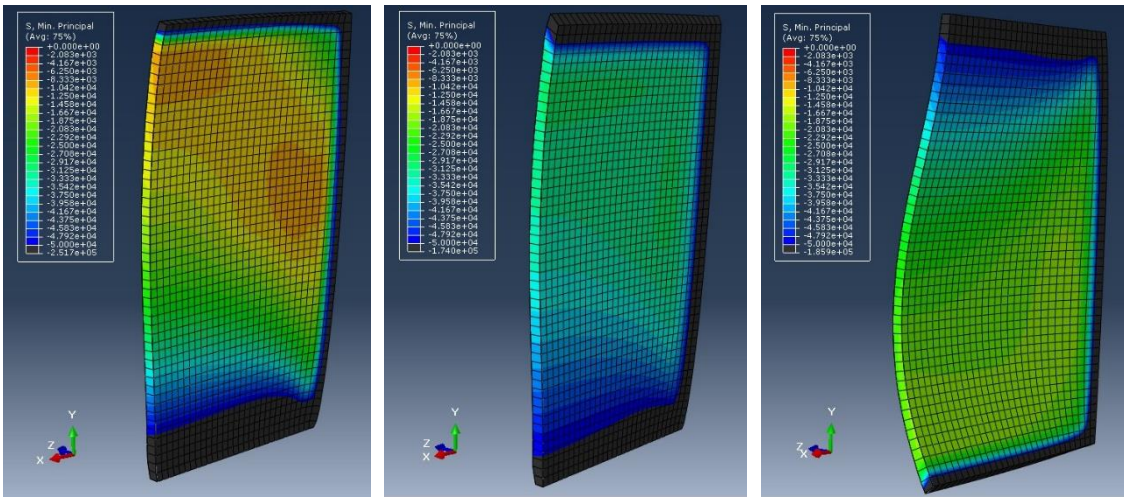

a) b) c)

Figure 25: Stresses distribution in the inner surface of the thermal insulation mortar after heating, using: a) Aerated concrete; b) Brick masonry; c) OSB.

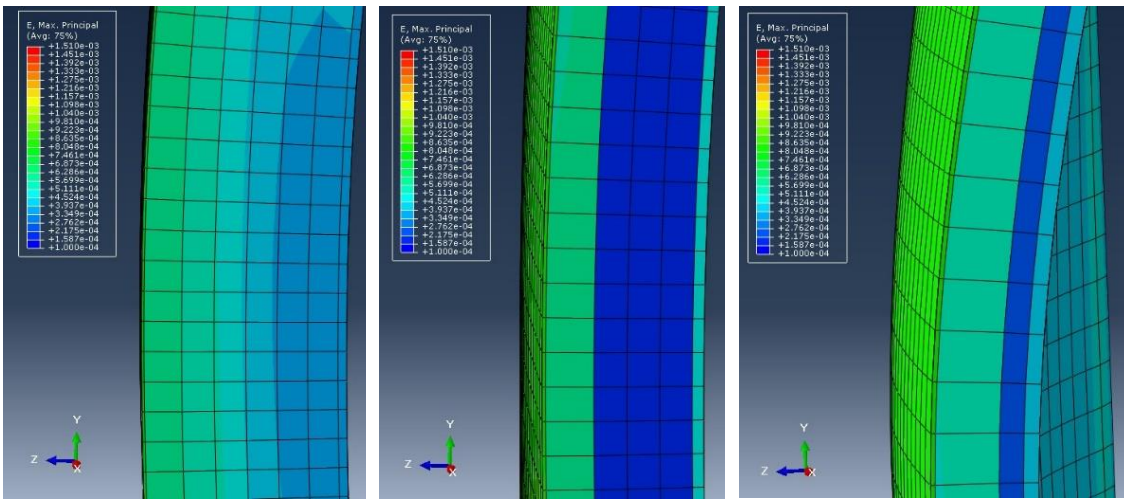

a) b) c)

Figure 26: Strains profile after heating, using: a) Aerated concrete; b) Brick masonry; c) OSB.

Observing the contraction period, the displacements are lower and similar using the heavier substrates, which was expected due to the low thickness of the OSB substrate. Regarding the strains profile in Figure 27, the walls using concrete masonry and OSB resulted in more significant strains in the thermal insulation layer.

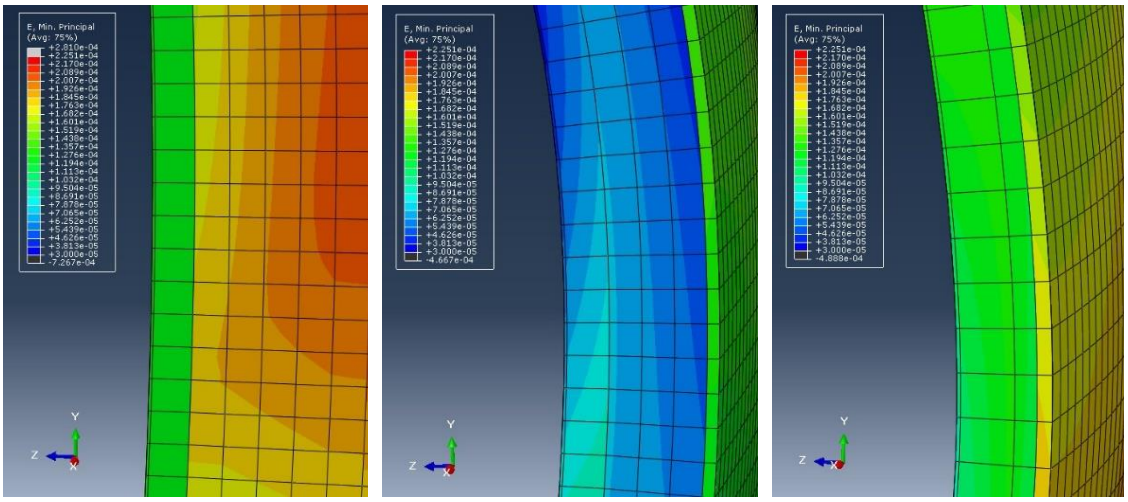

a) b) c)

Figure 27: Strains profile after the abrupt decrease, using: a) Aerated concrete; b) Brick masonry; c) OSB.

4. Thermo-energetic assessment

4.1. Framework and simulation model

The growing concern for energy efficiency and the environmental impact of buildings has driven the development of simulation tools that enable a more accurate assessment of building energy performance. In this context, EnergyPlus has emerged as a powerful and versatile tool for the energy simulation of buildings, alongside DesignBuilder, an interface software that runs EnergyPlus.

The primary objective of the current study was to evaluate the thermo-energetic performance of the new SIP panel, incorporating the new core formulation (SIP (ART)), and to compare it with a traditional SIP panel (SIP (EPS)).

The selected model for the study is a case study prototype of a nearly Zero Energy Building (nZEB), located in the student park of FEUP - Faculty of Engineering of the University of Porto, built in 2019. The prototype was constructed based on Light Steel Frame (LSF) and Structural Insulated Panels (SIP) technologies in collaboration with Dreamdomus. Figure 28 illustrates the modelling of the prototype using the DesignBuilder software.

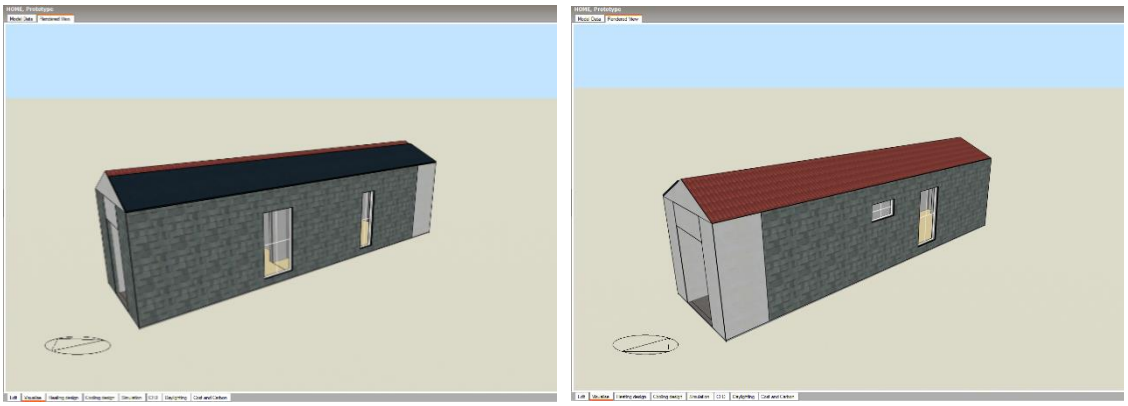

a) b)

Figure 28: 3D model on the DesignBuilder. a) North façade; b) South façade.

This model was selected to enable the application of the SIP (ART) system in future studies and experimentally validate the obtained results. The prototype consists of a single floor containing three rooms: a living room + kitchen, a bedroom, and a bathroom. The dwelling features a rectangular geometric configuration, with approximate dimensions of 11.0 m x 3.2 m and a ceiling height of 2.5 m. The living room + kitchen, bedroom, and bathroom have respective usable areas of 13.50 m², 10 m², and 3.30 m². Figure 29 depicts the floor plan of the prototype used in this case study.

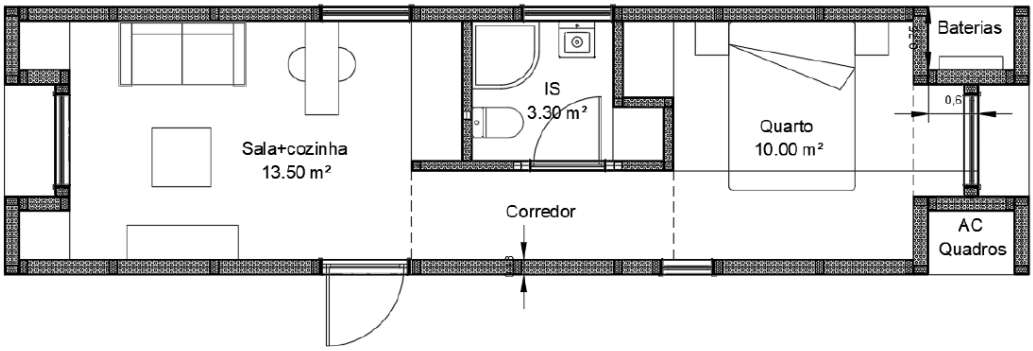

Figure 29: Floor plan of the model for the DesignBuilder.

Thus, two construction solutions were adopted at the building envelope level. As previously mentioned, a SIP with a core composed of the innovative mortar (ART) was introduced for comparison with the SIP composed of EPS. The characterisation of the roof and floor remained

unchanged from the previous case study. Table 6 summarises all the input parameters in DesignBuilder for the composition of materials and building elements.

Table 6: Material properties for the thermo-energetic simulation.

Element	Material	Thickness [m]	Thermal conductivity [W/m.°C]	Bulk density [kg/m³]	Specific heat [J/kg.°C]
Wall (ART)	Permeable membrane	0.01	1.0	1000	1000
	OSB	0.0200	0.105	650	1880
	ART	0.25	0.103	644	1111
	OSB	0.0127	0.105	650	1880
	Gypsum board	0.0125	0.25	900	1000
Wall (EPS)	Permeable membrane	0.01	1.0	1000	1000
	OSB	0.0200	0.105	650	1880
	EPS	0.097	0.04	15	1440
	OSB	0.0127	0.105	650	1880
	Gypsum board	0.0125	0.25	900	1000
Roof	Air gap				
	OSB	0.0127	0.13	650	1700
	Mineral wool	0.0800	0.037	35	1030
	Gypsum board	0.0125	0.25	900	1000
Floor	OSB	0.0127	0.13	650	1700
	Mineral wool	0.0400	0.038	150	1450
	OSB	0.0250	0.13	650	1700
	Wood	0.0200	0.13	500	1600

The exterior climate is selected based on the building's location, which typically corresponds to a predefined weather data file within the program.

The "Activity" tab in the DesignBuilder software defines indoor environmental conditions. Therefore, the program allows for the specification of occupancy type, the number of occupants per square meter, and the occupancy profile of the building. In this manner, a value of 0.03 persons per square meter was defined, translating to a two-person occupancy within the dwelling. The fresh air supply rate to be provided to the occupants is 10 l/s. The building's occupancy profile was developed to resemble real-life scenarios closely. The building is occupied from 18:00 to 9:00, Monday to Friday, and remains occupied around the clock during the weekend.

It is also possible to define the desired maximum and minimum setpoint temperatures, commonly referred to as "reference temperatures," that the building's HVAC system should maintain during occupied hours. Additionally, there is an option to specify limit temperatures for periods when the building is unoccupied, known as "setback temperatures." This measure aims to prevent excessive cooling during the night (in winter) or heating during unoccupied periods (in summer). This is crucial to ensure that high consumption of heating or cooling is not required at the beginning of the operating hours. As such, the heating and cooling setpoint temperatures were defined as 20°C and 25°C, respectively. The corresponding setback temperatures were established at 12°C and 28°C. These settings help regulate the indoor temperature effectively, optimising energy consumption and ensuring occupant comfort.

Furthermore, it is also possible to input internal gains from equipment usage. Once again, to align the model with reality, the following equipment items were taken into account:

- Refrigerator (400W)
- Washing machine (550W)
- Electric stove (1000W)
- Computer (30W)

The refrigerator, washing machine, and electric stove were placed in the "kitchen" space, while the computer was placed in the "bedroom" space. It was assumed that the refrigerator operates continuously throughout the year, whereas the washing machine is considered to be used as needed. These equipment-related gains contribute to the overall thermal dynamics of the building, influencing its energy performance and indoor thermal conditions.

The HVAC (Heating, Ventilation, and Air Conditioning) systems of any dwelling ensure thermal comfort throughout the year. For this reason, they hold great significance, as the energy needs for heating and cooling the building will be calculated. As such, it is imperative to have knowledge of the operating period, select the energy source, and determine the corresponding COP (Coefficient of Performance). While the specific COP value isn't required to proceed with the simulation, it aids in making the simulated equipment closely resemble reality. Hence, the heating and cooling energy output values do not represent the energy demanded by the HVAC systems; instead, they represent the energy needed to be supplied to the indoor air to achieve system equilibrium. The heating system was configured with the electric grid as the energy source. The

system's efficiency is set at 100%, and it operates from 8:00 pm to 9:00 pm from Monday to Friday and operates 24 hours on weekends.

To model the cooling system closer to reality, a COP value of 4.0 was defined, and the energy source was chosen as the electric grid. The operating period is the same as the heating system.

For ventilation characterisation, both natural and mechanical ventilation were considered. For natural ventilation, an operating period of 2 hours every day of the week was established, with an air change rate of 3.0 changes per hour (ACH). An ACH of 0.6 was considered for mechanical ventilation, assuming a system that operates continuously 24 hours a day, seven days a week. The air permeability value was set at 0.55. These ventilation parameters are crucial in assessing the building's indoor air quality and energy consumption.

The simulations were conducted for the northern orientation and across three distinct climates (Porto, Bordeaux, and Helsinki), as previously specified. Additionally, solar absorption coefficients for white (0.27) and black (0.88) surfaces were considered.

Consequently, two simulation scenarios were formulated:

Case 1 - HVAC Systems and Equipment OFF: in this scenario, the objective is to evaluate the dwelling while disregarding the presence of HVAC systems and equipment. One of the analyses assesses the fluctuation between external and operative temperatures within the dwelling for both SIP (EPS) and SIP (ART) systems across various climates. Consequently, the number of hours of thermal discomfort will also be evaluated.

Case 2 - HVAC Systems and Equipment ON: within this scenario, the dwelling is evaluated with fully operational HVAC systems and equipment. The principal aim is to scrutinise variations in the overall energy demands of the dwelling under diverse climatic conditions. This includes considering the goals established in the preceding scenarios, such as the thermal discomfort assessment and SIP systems' thermal behaviour.

Case 2 also provides the means to assess the impact of activated HVAC systems and equipment on the dwelling's thermal and energy performance in comparison to Case 1, where these systems are inactive.

These simulation scenarios and the ensuing analyses provide a comprehensive framework for juxtaposing the performance of SIP (EPS) and SIP (ART) systems across various climatic conditions. This investigation offers valuable insights into these systems' thermal and energy dynamics, shedding light on their effectiveness in maintaining thermal comfort and reducing energy consumption.

4.2. Case 1

The primary objective of this analysis is to assess the relationship between external temperatures and operative temperatures of SIP (EPS) and SIP (ART) systems at each location. This evaluation examines thermal comfort and discomfort hours, gauging these systems' performance. Notably, the dashed lines on the graphs depict the maximum and minimum values considered acceptable to ensure occupants' comfort conditions within the building.

The maximum value is set at 25°C, while the minimum value for winter conditions is established at 20°C. These reference lines serve as benchmarks for scrutinising the suitability of indoor temperatures concerning residential comfort standards. Through this approach, the study aims to provide insights into SIP systems' thermal behaviour and effectiveness, facilitating an informed assessment of their capacity to maintain occupant comfort and mitigate thermal discomfort.

Observing Figure 30, it becomes evident that in the absence of heating and cooling systems, the variations in indoor air temperature exhibit significant discrepancies, surpassing the comfort threshold.

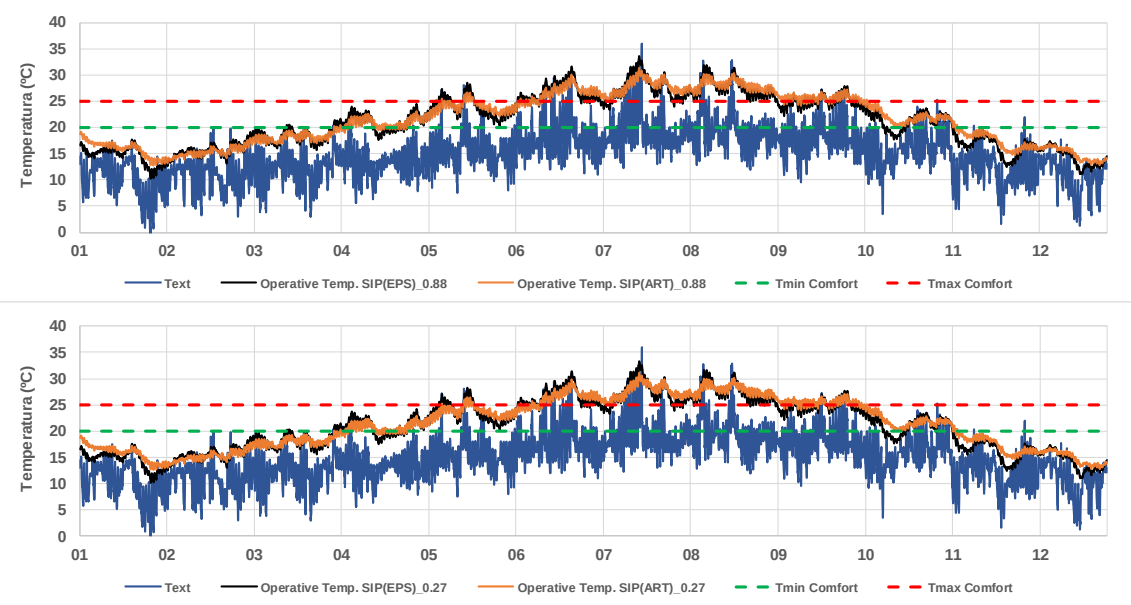

Figure 30: Hourly temperature variation in Porto for α=0.27 (above) and α=0.88 (below), considering a simulation period of 12 months – Case 1

It is observable that for a coefficient of 0.27, SIP(EPS) exhibits a slightly higher number of hours within the thermal comfort range compared to SIP(ART), i.e., SIP(EPS) has 2398 hours while SIP(ART) has 2386 hours within the comfort interval. Conversely, SIP(ART) presents a relatively similar number of hours for a darker absorption coefficient to SIP(EPS).

Regarding the variation of outdoor temperatures, the climate in Bordeaux is similar to that of Porto, except that Bordeaux experiences lower minimum temperatures. It can be observed in Figure 31 that both SIP(EPS) and SIP(ART) exhibit the same variation in operative temperatures throughout the year. From January to April, internal temperatures remain below the lower comfort limit (20°C), with SIP(EPS) reaching slightly lower values than SIP(ART). From June to mid-September, the operative temperatures of both systems exceeded 25°C, with SIP(EPS) reaching slightly higher values, although not significantly so.

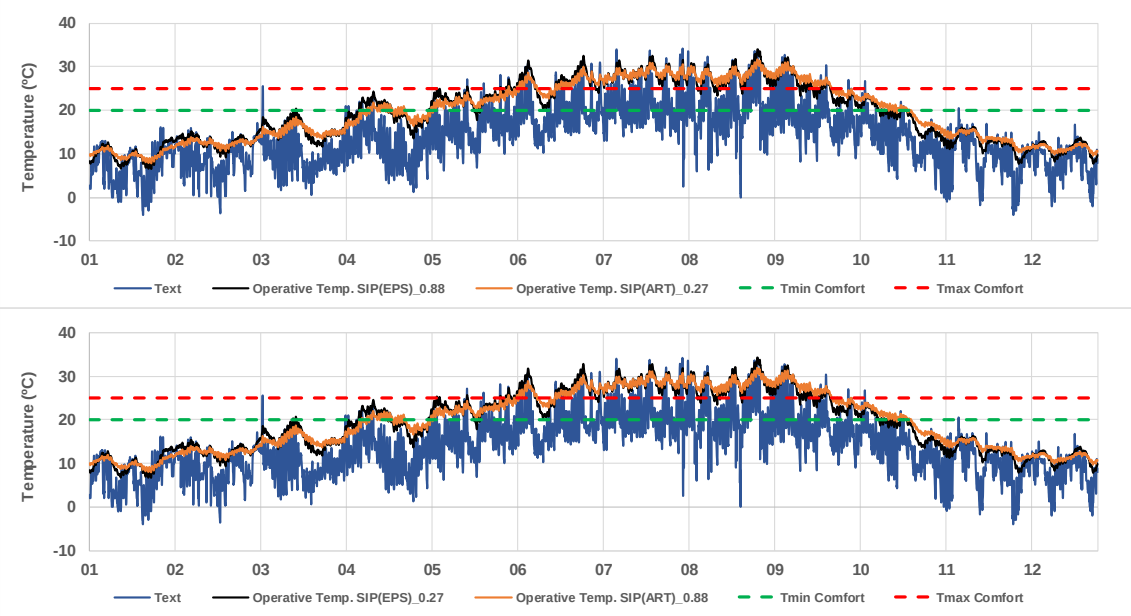

Figure 31: Hourly temperature variation in Bordeaux for α=0.27 (above) and α=0.88 (below), considering a simulation period of 12 months – Case 1

Figure 32 shows variations in outdoor temperature and operative temperature for the Helsinki climate, as well as for the SIP(EPS) and SIP(ART) systems, are evident. The Helsinki climate is characterised as cold, with outdoor temperatures remaining below the minimum comfort limit (20°C) for a significant part of the year. Only during the summer months are temperatures recorded approaching the maximum comfort limit (25°C). SIP(ART) exhibited slightly lower operative temperatures from January to April than SIP(EPS). From June to mid-September, operative temperatures for both systems fluctuated between 20°C and 25°C, with SIP(EPS) reaching slightly higher values, although not significantly so. Starting in September, the scenario reverses, with SIP(ART) showing slightly higher operative temperatures than SIP(EPS), contrary to the observations in the first third of the year.

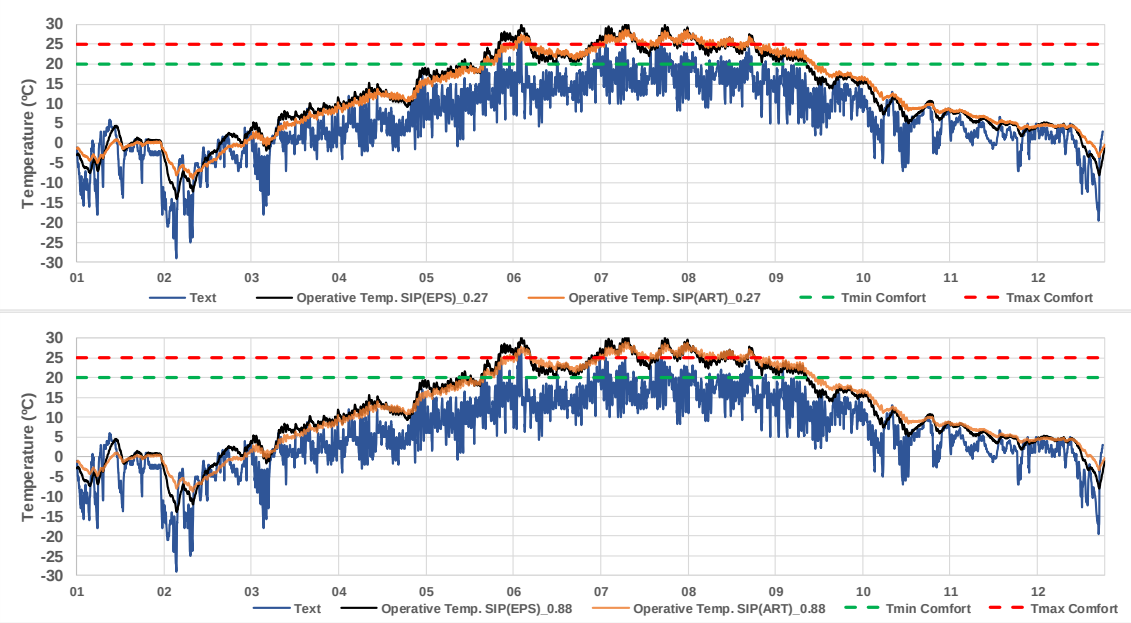

Figure 32: Hourly temperature variation in Helsinki for α=0.27 (above) and α=0.88 (below), considering a simulation period of 12 months – Case 1

It is possible to conclude that SIP(EPS) achieves slightly higher maximum interior temperatures and lower minimum interior temperatures than SIP(ART). Once again, these results can be attributed to the higher thermal effusivity of the mortar compared to EPS. In summary:

- SIP(EPS) has a more significant number of hours within the comfort zone compared to SIP(ART) for the Porto, Bordeaux, and Helsinki climates;
- There are more hours for absorption of 0.27, where the operative temperature remains within comfort limits;
- SIP(ART) shows a greater number of hours where T > 28°C for the Porto and Bordeaux climates, but for the Helsinki climate, there is a decrease;
- SIP(ART) presents a higher number of hours where T < 12°C for the Porto and Bordeaux climates, but for the Helsinki climate, there is a decrease.

4.3. Case 2

For Case 2, as mentioned earlier, the HVAC systems and equipment were activated. The equipment includes a refrigerator, an electric heater, a washing machine, and a computer. This

analysis aims to assess the number of hours spent in thermal comfort and discomfort for both SIP(EPS) and SIP(ART) systems in each location and their heating and cooling energy requirements.

As shown in Figure 33, the observed fluctuation in operative temperature during the summer months, frequently exceeding 25°C, is a result of considering that the HVAC systems would only be operational during the dwelling's occupancy period (18:00 to 9:00). Consequently, during the day and the hours of higher outdoor temperature, the dwelling remains unconditioned, leading to an elevation in operative temperature. SIP(EPS) and SIP(ART) exhibit a similar variation in operative temperatures throughout the year. From January to April, internal temperatures remain within the thermal comfort range. From June to October, operative temperatures for both systems exceeded 25°C, with SIP(EPS) reaching slightly higher values, though not significantly so.

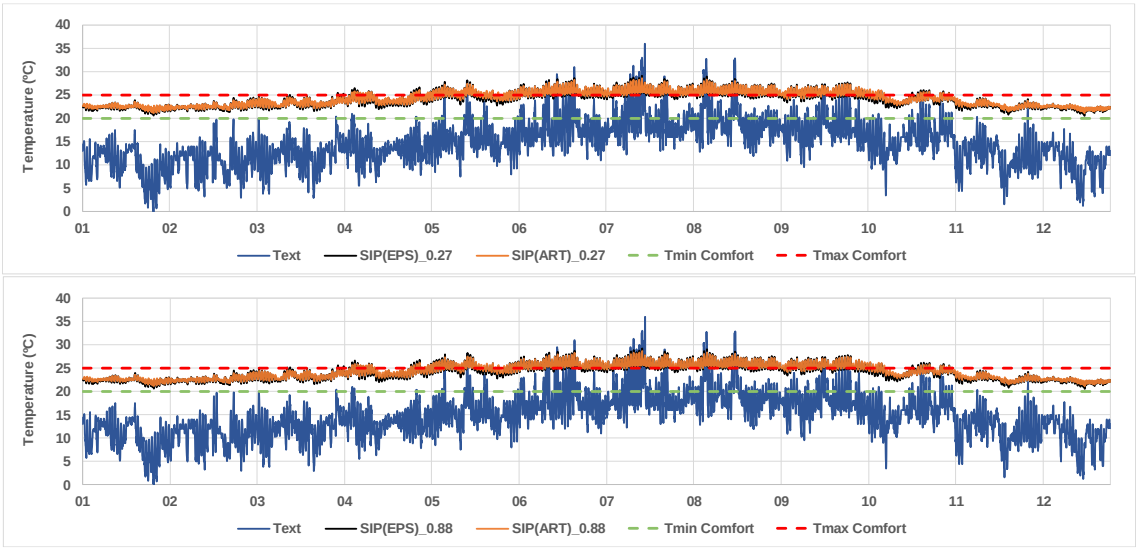

Figure 33: Hourly temperature variation in Porto for α=0.27 (above) and α=0.88 (below), considering a simulation period of 12 months – Case 2

In Figure 34, the cooling and heating energy requirements for SIP(EPS) and SIP(ART) systems are graphically depicted. It is evident from the graph that SIP(ART) exhibits lower cooling and heating energy demands compared to SIP(EPS).

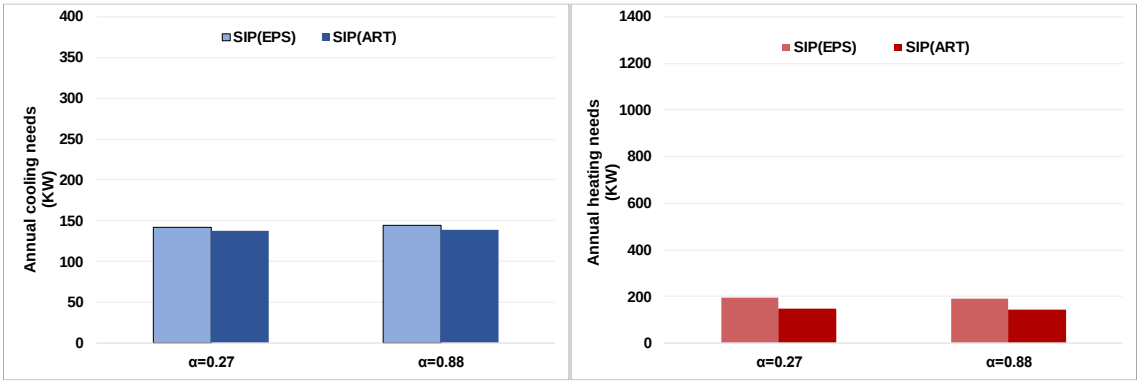

Figure 34: Cooling (blue, left) and heating (red, right) needs of SIP (EPS and SIP (ART) in Porto – Case 2

It can be observed that the SIP(ART) system exhibits a total energy consumption of 283.97 kWh/year and 280.72 kWh/year for coefficients of 0.27 and 0.88, respectively. Consequently, there is no significant energy difference between light-coloured and dark-coloured coefficients. Hence, the annual energy consumption difference between SIP(EPS) and SIP(ART) is approximately 50 kWh/year.

Figure 35 shows the variations in exterior temperature and operative temperature for the Bordeaux climate in both the SIP(EPS) and SIP(ART) systems, considering solar absorption coefficients representing white (α=0.27) and black (α=0.88). In terms of variations in operative temperatures, the Bordeaux climate exhibits a similar pattern to the Porto climate, whereby both SIP(EPS) and SIP(ART) remain below 25°C and above 20°C during the first and last thirds of the year. Throughout the summer months, the operative temperatures of both systems surpass 25°C, with SIP(EPS) achieving slightly higher values, but only marginally so.

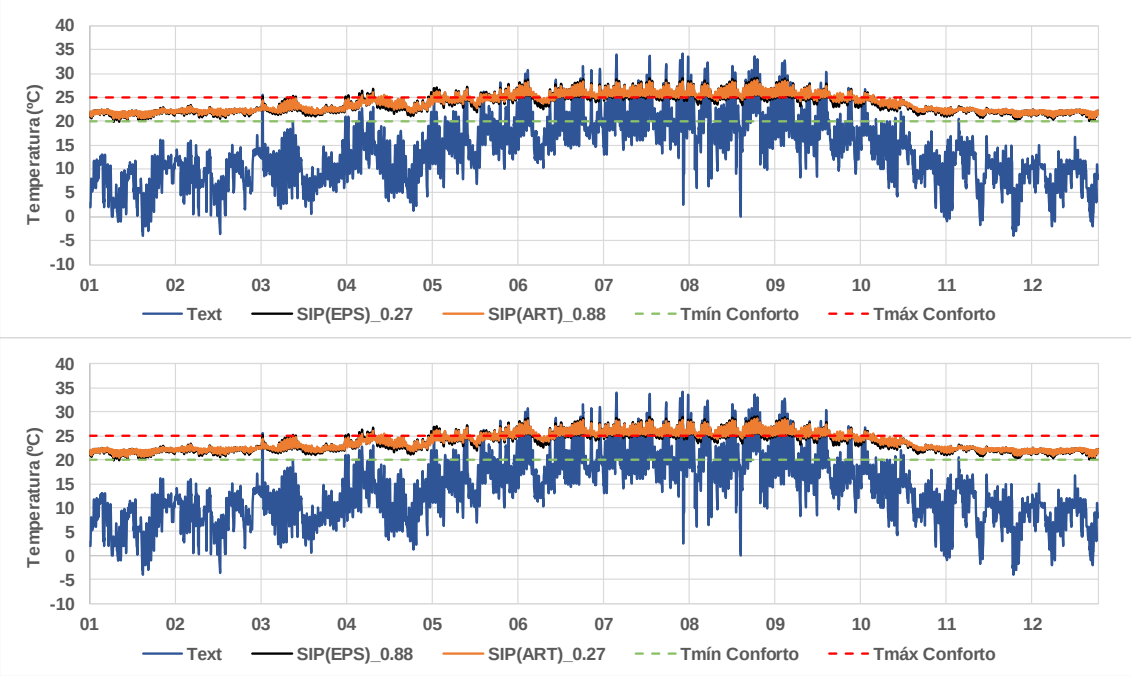

Figure 35: Hourly temperature variation in Bordeaux for α=0.27 (above) and α=0.88 (below), considering a simulation period of 12 months – Case 2

The energy requirements for cooling and heating are graphically illustrated in Figure 36, from which we can infer that SIP(ART) exhibits lower heating energy demands while concurrently displaying higher cooling energy requirements compared to SIP(EPS).

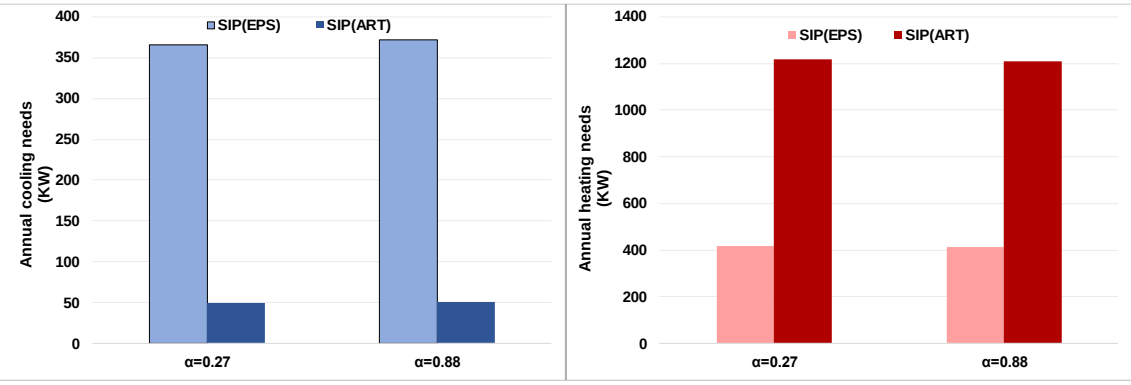

Figure 36: Cooling (blue, left) and heating (red, right) needs of SIP (EPS and SIP (ART) in Bordeaux – Case 2

Figure 37 shows the variations in exterior temperature and interior temperature for the Helsinki climate and the SIP(EPS) and SIP(ART) systems. Upon analysing Figure 81, it becomes evident that

SIP(ART), from January to March, exhibits significantly lower operable temperatures than SIP(EPS). Furthermore, SIP(ART) demonstrates pronounced oscillations in interior temperature, whereas SIP(EPS) displays a more consistent variation. From June to mid-September, the operable temperatures of both systems exceeded 25°C, with SIP(EPS) slightly surpassing the values. From September onwards, the pattern observed in the first third of the year is repeated, except for the more steady variation in SIP(ART).

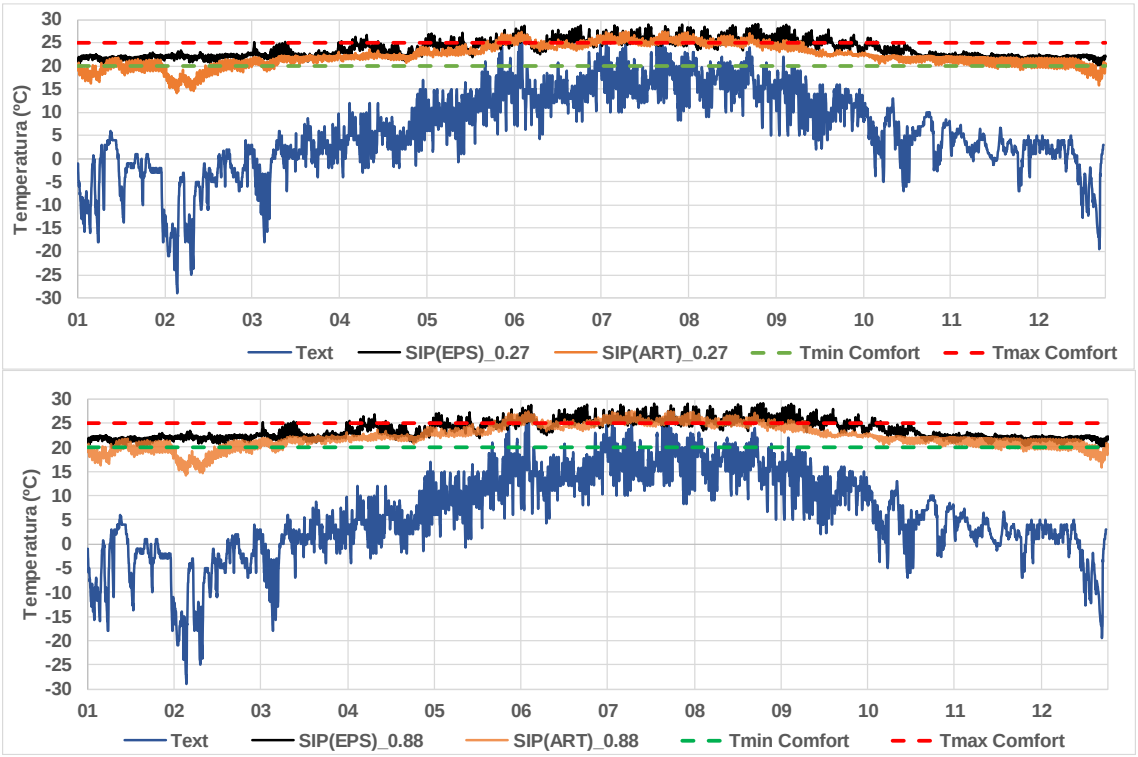

Figure 37: Hourly temperature variation in Helsinki for α=0.27 (above) and α=0.88 (below), considering a simulation period of 12 months – Case 2

The energy requirements for heating and cooling are graphically depicted in Figure 38, revealing that SIP (ART) demands higher heating energy but lower cooling energy compared to SIP (EPS).

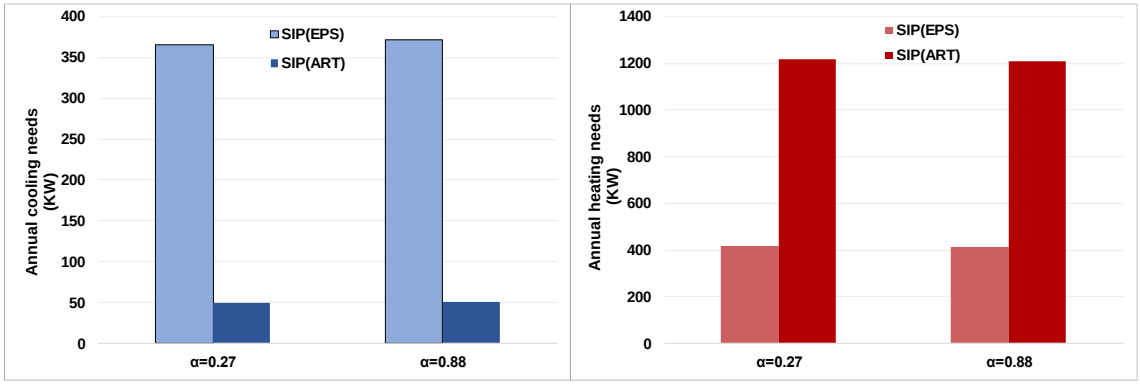

Figure 38: Cooling (blue, left) and heating (red, right) needs of SIP (EPS and SIP (ART) in Helsinki – Case 2

It can be observed that SIP(ART) exhibits total energy requirements of 1267 kWh/year and 1260 kWh/year for α=0.27 and α=0.88, respectively. Out of these total values, approximately 1200 kWh/year arise from heating needs, with only 50 kWh/year attributed to cooling requirements. In contrast, SIP (EPS) manifests total energy demands of 784 kWh/year and 786 kWh/year for α=0.27 and α=0.88, respectively. Among these values, around 420 kWh/year stem from heating needs, while 365 kWh/year pertain to cooling necessities. Consequently, SIP(ART) showcases an increase of approximately 480 kWh/year in total energy requirements compared to SIP (EPS). In summary:

- SIP (EPS) exhibits more hours within the comfort zone than SIP (ART) for the Porto, Bordeaux, and Helsinki climates;
- There is a higher quantity of hours for absorption of 0.27, where the operative temperature remains within comfort limits.;
- SIP (ART) demonstrates a higher number of hours where T>28 ºC for Porto, Bordeaux, and Helsinki climates;
- SIP (ART) displays lower heating and cooling energy requirements for the climates of Porto and Bordeaux;
- SIP (ART) presents triple the heating energy demand of SIP (EPS), yet in terms of cooling demand, it only accounts for 1/6 of SIP (EPS) requirements.